

# Measurements and Macro Models of Ionomeric Polymer-Metal Composites (IPMC)

Xiaoqi Bao, Yoseph Bar-Cohen, Shyh-Shiuh Lih  
Jet Propulsion Lab, California Institute of Technology  
4800 Oak Grove Dr., MS 67-119, Pasadena, CA, USA 91109-8099  
[xbao@jpl.nasa.gov](mailto:xbao@jpl.nasa.gov); phone 1-818-354-0298; <http://ndeaa.jpl.nasa.gov>;

## ABSTRACT

Ionomeric Polymer-Metal Composites (IPMC) are attractive type of electroactive polymer actuation materials because of their characteristics of large electrically induced bending, mechanical flexibility, low excitation voltage, low density, and ease of fabrication. The diffusion of ions between the electrodes causes the material to bend. The unique features of the IPMC materials and their need for special operating environment require new approaches to measuring their characteristics. A macro model that relates the electric input and mechanical output is required for the material characterization and application. This paper addresses the macro models for the electric inputs and electromechanical actuation of IPMC. A distributed RC line model is developed to describe the 'varying capacitance' of the electric input behavior and a four-parameter model to express the relaxation phenomena. The power capacities of the IPMCs are estimated according to the established models and the measured results. Results for several types of IPMCs, which present different behaviors, are presented.

**Keywords:** Electroactive Polymer, EAP, Ionomeric Polymer-Metal Composite, IPMC, Actuators, Macro Model, Material Characterization.

## 1. INTRODUCTION

Electroactive polymers (EAP), which are an emerging class of actuation materials, have many attractive characteristics<sup>1</sup>. Implementing these materials as actuators requires the availability of properties database and scaling laws to allow actuator or transducer designers to determine the response at various operation conditions. A metric is needed for the comparison of the properties of these materials with other electroactive materials and devices to allow impartial comparison of the performance of the various materials<sup>2</sup>. In selecting characterization techniques it is instructive to look at the various Electroactive Polymers and the source of their strain-field response. Two main classes can be identified: Electronic and Ionic. The emphasis of this paper is on IPMC that is a part of the ionic EAP materials category. These materials usually contain an electrolyte and they involve transport of ions/molecules in response to an external electric field. Examples of such materials include conductive polymers/polyaniline actuators, IPMC, and ionic gels. The field controlled migration or diffusion of the various ions/molecules results in an internal stress distribution. In some conductive polymers the materials exhibit both ionic and electronic conductivity. These materials are relatively new as actuator materials and have received much less attention in the literature than the piezoelectric and electrostrictive materials. At present, due to a wide variety of possible materials and conducting species, no generally accepted phenomenological model exists and much effort is underway to determine the commonalties of the various materials systems. A clearer understanding of the characterization techniques would help immensely in determining underlying theories and scaling laws for these actuator materials.

The unique behaviors of the IPMC introduced new challenges to material evaluation and characterization. An experimental setup was developed at NDEAA Lab, JPL<sup>3</sup>. The setup, equipped with high speed CCD camera and controlled by computer, acquired 2-D images of the IPMC strips that were subjected to various electric excitations and input voltage/current. Data processing software was used to extract the displacement and curvature of IPMC as a function of time. Sample strips were immersed in water to minimize the effect of moisture content and were tested with and without tip mass loading. In order to avoid electrolysis, the applied voltages were usually limited to 1-V with either positive or negative polarity.

This paper focuses on the macro models for electric inputs and electromechanical actuation of IPMC. The macro models that relate the electric input and mechanical output are required for the material characterization i.e. to define and extract the material parameters in order to support potential application establishing a mathematical base for actuator design. A distributed RC line model is developed to describe the 'varying capacitance' of the electric input behavior and a four-parameter model to express the relaxation phenomena. The power capacities of the IPMCs are estimated according to the established models and the measured results.

## 2. ELECTRIC INPUT MODEL

### 2.1 Clumped RC model for input current/voltage response of IPMC

The IPMC has two parallel electrodes and electrolyte between the electrodes. Double-layer capacitors are formed on the interfaces of two electrodes and the electrolyte. The electrolyte between the electrodes may introduce an internal resistance. This series circuit of C-R-C can be simplified to R-C circuit. Plus the possible leakage, a (R-C)||R circuit was constructed as presented in Fig. 1, where  $r_0$  is the internal resistance of the voltage source. Under step voltage  $V$ , the response of input current is derived as

$$I(t) = \frac{V}{r_0 + r_2} \left[ 1 + \left( \frac{r_1 + r_2}{R} - 1 \right) e^{-\alpha t} \right], \quad (1)$$

where

$$R = r_1 + \frac{r_0 r_2}{r_0 + r_2} \quad \text{and} \quad (2)$$

$$\alpha = \frac{1}{RC}. \quad (3)$$

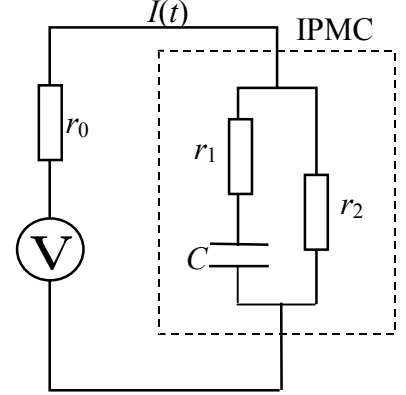


Fig. 1: Clumped RC model for input response

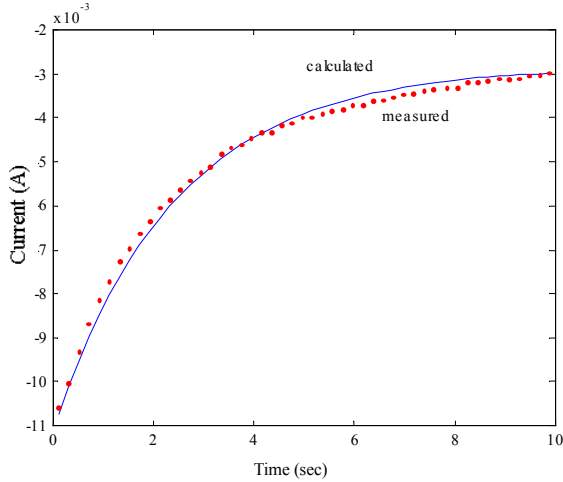


Fig. 2: Time response of input current of a  $\text{Li}^+$ /Nafion sample,  $\cdots$  measured data,  $\text{—}$  model fitted curve.

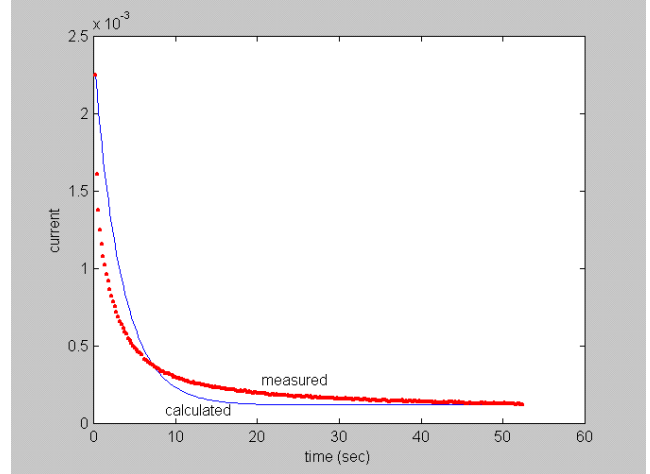


Fig. 3: Time response of input current of a  $\text{TBA}^+$ /Flemion sample,  $\cdots$  measured data,  $\text{—}$  model fitted curve.

This model was utilized to fit the experimental data with three adjustable parameters of  $r_1$ ,  $r_2$  and  $C$ . The model fits some data well. An example is presented in Fig. 2. The sample is a  $\text{Li}^+$ /Nafion IPMC strip made by ERI with sizes of  $30 \times 3 \times 1$  mm. The parameters determined by the best fitting are  $r_1=232\Omega$ ,  $r_2=700\Omega$ , and  $C=10000\mu\text{F}$ .

Another result is shown in Fig. 3. The sample is a  $\text{TBA}^+$ /Flemion IPMC strip made by AIST with sizes of  $32 \times 3.4 \times 0.17$  mm. The parameters determined by the best fitting are  $r_1=340\Omega$ ,  $r_2=8280\Omega$ , and  $C=7580\mu\text{F}$ . A quite large difference between the model and the experimental curves is observed suggesting that there is a need to develop a distributed model as discussed in the next section.

### 2.2 Distributed RC model for input current/voltage response of IPMC

As shown in Fig. 3, the clumped RC model could not fit the time response well for input current for the AIST sample. The experimental curve shows a faster drop of current at the beginning than the model predicted. It implies that the capacitance

seems increasing with the time. Actually a formula of  $I(t) = a + b(t - t_0)^{-0.45}$  fits the experiment much better as shown in Fig. 4. Other researchers<sup>4</sup> also reported similar phenomena that the capacitance of IPMC sample was “varying” with the rising time of the applied voltage, from  $400\mu\text{F}/\text{cm}^2$  at  $1\text{V}/\text{s}$  to  $1300\mu\text{F}/\text{cm}^2$  at  $0.1\text{V}/\text{s}$  for  $\text{Li}^+/\text{Flemion}$ .

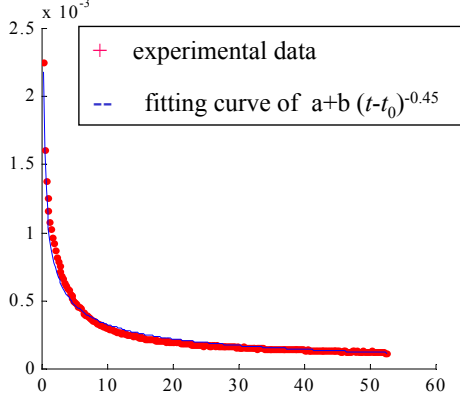


Fig. 4: Time response of input current of the TBA+/Flemion sample fitted by formula of  $I(t) = a + b(t - t_0)^{-0.45}$

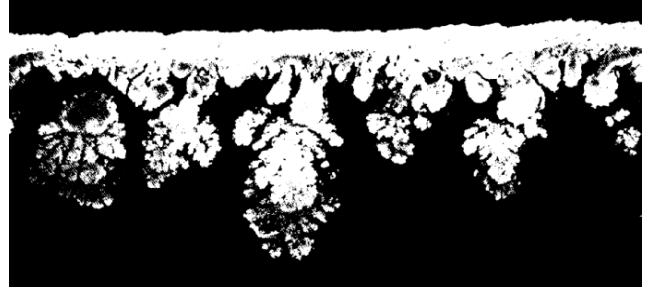


Fig. 5: SEM micrograph showing fractal-like structure of a gold electrode, provided by AIST.

However, there is no reason for the double-layer capacitances in the IPMC to vary. Actually, the electrode on the IPMC are not a simple uniform metal layer. The microstructure of the electrode strongly depends on the process of fabrication. Details of an electrode made by AIST show in Fig.5. The electrode having a fractal-like structure diffuses into the polymer. The surfaces of electrode s have unequal paths to the electric source and for the ions diffusion. As a result, there is the formation of double-layer capacitances associated with different resistances, which may behave like a “varying” capacitance.

For example, considering a tree-like fractal structure as show in Fig. 6, the stickers in the next level are averagely scale down by ratio of  $\beta$  and number increased by fact of  $m$ . We roughly have

$$C_{n+1} = m\beta^2 C_n$$

$$r_{n+1} = \frac{r_n}{m\beta}$$

where  $C_n$  is the capacitance associated with the stickers in level  $n$  and  $r_n$  is the resistance between level  $n+1$  and level  $n$ . The forms of these formulas may change according to the form of the fractal structure. Each level associated with a capacitance and connected each other in sequence by corresponding resistance.

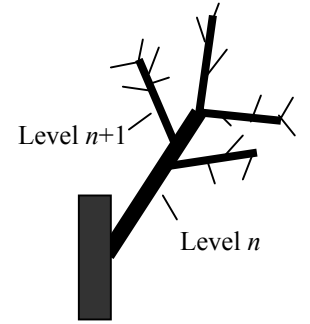


Fig. 6: Tree-like fractal structure

(5)

We constructed a circuit model to present the double-layer capacitance of the fractal-like electrode as show in Fig. 7. The fractal structures actually have random nature and cannot define the level number clearly. Therefore, we consider the model is a distributed RC line rather than a discrete network. The resistances in the circuit represent resistances both in the metal of electrode and, maybe more significantly, in the ionomeric polymer.

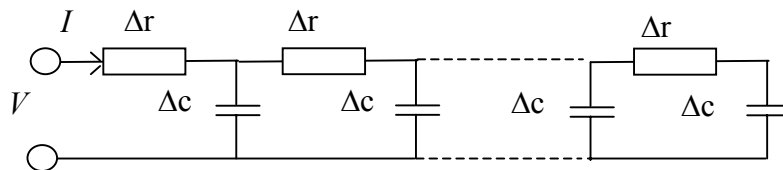


Fig. 7: Distributed RC line model for fractal-like electrode in IPMC

The partial differential equation of this distributed RC line is derived as

$$\frac{\partial V}{\partial t} = Z_c^2 \frac{\partial^2 V}{\partial r^2}, \quad (6)$$

where

$$Z_c^2(r) = 1 / \frac{dC}{dr}. \quad (7)$$

In the simplest case of  $Z_c(r)$  being constant, the equation has explicit general solution as

$$V(r, t) = c_1 e^{st - \sqrt{sr}/Z_c} + c_2 e^{st + \sqrt{sr}/Z_c} + c_3 \quad (8)$$

and corresponding current is as

$$I(r, t) = c_1 \frac{\sqrt{s}}{Z_c} e^{st - \sqrt{sr}/Z_c} - c_2 \frac{\sqrt{s}}{Z_c} e^{st + \sqrt{sr}/Z_c}. \quad (9)$$

Furthermore, if the line is infinite, we find the response of input current for step voltage input as

$$I(0, t) = \frac{V_0}{2Z_c \pi j} \int_{\sigma - j\infty}^{\sigma + j\infty} \frac{e^{st}}{\sqrt{s}} ds = \frac{V_0}{Z_c \sqrt{\pi t}}, \quad (10)$$

while assuming the voltage on all capacitors is zero at beginning. This result shows the current response decreases with time as  $t^{-0.5}$  compared to the best fit of the experimental data as  $t^{-0.45}$  as shown in Fig. 4. It implies that this distributed RC line may be a more accurate model than the clumped RC model.

The distributed model shown in Fig. 7 presents the electrode. The leakage resistance, the counterpart of  $r_2$  in the clumped RC model, and the resistance of the electrolyte layer between the two electrodes, the counterpart of  $r_1$  in the clumped RC model, should be added to form the complete input model of IPMC with this type electrodes. In addition,  $Z_c(r)$  is a variable in general and the line may have limited total capacitance. We expect that the final model will fit the experimental data more closely.

### 3. ANALYTICAL MODEL FOR ELECTROMECHANICAL ACTUATION

#### 3.1 Electromechanical response and relaxation

Studies indicate that the response of IPMC strongly depends on its backbone polymer and ionic content<sup>5,6</sup>, especially the counter ion. Basically, they can be divided to two categories based on their cations size, (a) Small cations such as  $\text{Li}^+$ ,  $\text{Na}^+$  and  $\text{K}^+$ , and (b) large cations such as alkyl ammonium ions. The typical actuation responses of these two types of IPMC are presented in Fig. 8 and 9. The IPMC with small cation of  $\text{Li}^+$  has a quick response to the applied voltage and a slow back relaxation. The IPMC with large cation of tetra-n-butylammonium<sup>+</sup> (TBA) responds slowly to applied voltage but with no relaxation. It is believed that the small cations move easier over the polymer backbone. The fast movement of the cations toward the cathode together with associated water molecular results in an initial quick bending toward to the anode. This response is followed with a relaxation that may be caused by water leakage resulting from a high-pressure layer near the cathode toward to the anode through channels in the polymer backbone. The process stops when water equilibrium is reestablished. On the contrary, large cations migrate significantly slower and present slow reaction to the electric field. Thus, no relaxation is

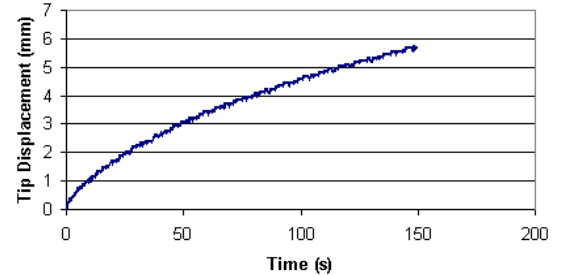
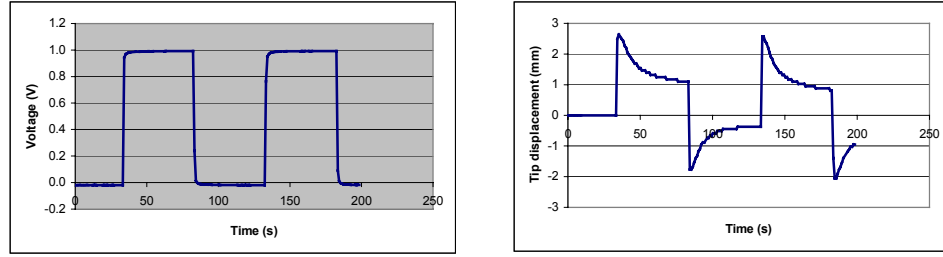


Fig. 8: Response of tetra-n- butylammonium/ Flemion

observed and it may be the result of the fact that the ions block the channels or the equilibrium with concentrated cations requires more water.



(a) Applied voltage

(b) Tip displacement

Fig. 9: Response of a  $\text{Li}^+$ /Nafion strip sample of  $25 \times 3 \times 0.19 \text{ mm}^3$  to 0V/1V square wave voltage

### 3.2 Model for IPMC with relaxation

We develop the model basically for the IPMC strip with relaxation and consider the IPMC without relaxation as a special case of the model.

Under a step voltage, after a very quick bending towards anode, the strip shows a slow relaxation towards cathode, indicating existence of two time constants. We constructed the model using the understanding of the possible underlying mechanism of the phenomena. We assume the positive ions bring more water to the cathode than the water they should be associated in equilibrium. There is a diffusion of the water back to the anode after initial moving to the cathode.

$$\frac{dk}{dt} = K_1 \frac{dq}{dt} - \frac{1}{\tau_2} (k - K_2 q), \quad (11)$$

where  $k$  is the curvature of the strip,  $q$  the electric charge,  $K_1$  is the coefficient for bending effect of the charge freshly moving to the electrode,  $K_2$  is the coefficient for bending effect of the charge in equilibrium state, and  $\tau_2$  is the relaxation time constant.

When the clumped RC circuit model can represent the electric input response of the sample, we use the model to calculate the electric charge on the electrode,

$$R \frac{dq}{dt} = V - \frac{q}{C}. \quad (12)$$

The solution for the step voltage is

$$q = VC(1 - e^{-t/RC}) = VC(1 - e^{-t/\tau_1}). \quad (13)$$

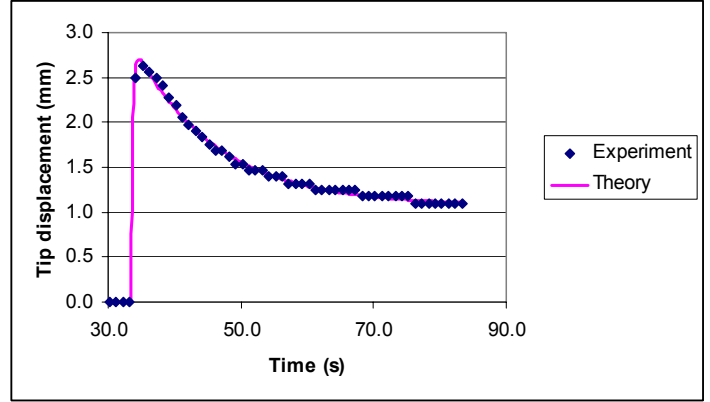
where  $\tau_1$  is time constant of the RC circuit which is equal to  $RC$ . Substituting Eq. (13) to Eq. (11) and assuming the initial condition  $k(0) = 0$ , we have

$$k = V(K_{V2} - \frac{K_{V1}\tau_2 - K_{V2}\tau_1}{\tau_2 - \tau_1} e^{-t/\tau_1} + \frac{\tau_2(K_{V1} - K_{V2})}{\tau_2 - \tau_1} e^{-t/\tau_2}), \quad (14)$$

Where  $K_{V1} = CK_1$  and  $K_{V2} = CK_2$ .

This model defines four-parameters of IPMC materials,  $K_{V1}$ ,  $K_{V2}$ ,  $\tau_1$  and  $\tau_2$ , which can be found by curve fitting with the experiment data. Fig. 10 shows the fitting results for the  $\text{Li}^+$ /Nafion strip. The theoretical curve conforms the experimental data very well. The parameters extracted are  $\tau_1 = 0.3 \text{ s}$ ,  $\tau_2 = 10.7 \text{ s}$ ,  $K_{V1}^t = 2.87 \text{ mm/V}$ ,  $K_{V2}^t = 1.07 \text{ mm/V}$ , where  $K_{V1}^t$  and  $K_{V2}^t$  are the coefficients of tip displacement over voltage corresponding to the  $K_1$  and  $K_2$  in Eq. (14).

Fig. 10: Comparison of the theoretic model with the experimental data of a Li<sup>+</sup>/Nafion strip from ERI.



When  $K_1 = K_2$ , this four-parameter model will reduce to a two-parameter model representing the actuation response without relaxation. The ordinary differential equation becomes

$$\frac{dk}{dt} = \frac{1}{\tau} (K_v - k). \quad (15)$$

The response for a step voltage is written as

$$k = VK_v (1 - e^{-t/\tau}). \quad (16)$$

It is the same as the model developed by K. Bhattacharya *et al*<sup>7</sup>.

#### 4. ESTIMATION OF POWER DENSITY

The developed macro actuation model established the relationship of the bending of the IPMC strip without mechanical load with the input voltage. To determine the loading capability, the knowledge of the bending rigidity or the equivalent Young's modulus are required. We obtained the equivalent Young's modulus by the best curve fitting of the solution of the model to the experimental data of the sample with known tip force. Then, the response of the strip with mechanical load can be found and the mechanical power output can be determined. The power output is a function of amplitude and waveform of the input voltage and the load. In the following power density estimation, we limited the input voltage as

- 1) the peak voltage  $\leq 2$  V;
- 2) harmonic waveform of variable frequency.

Only quasi-static actuation is considered, that is, no resonance phenomena is involved.

For the IPMC without relaxation, the power density of the material can be estimated according to Eq.(15). Under harmonic voltage driving of  $V(t) = Ve^{j\omega t}$ , we have

$$k = \frac{K_v V}{1 + j\omega\tau}. \quad (17)$$

The voltage induced a momentum of

$$M_v = kEI = EI \frac{K_v V}{1 + j\omega\tau} \quad (18)$$

to the strip. If there is a mechanical momentum resistance  $M_L = j\alpha EIk$  on the strip, the equation becomes

$$EI k = M_v - M_L = EI \frac{K_v V}{1 + j\omega\tau} - j\alpha EI k. \quad (29)$$

The curvature can be solve and the power to momentum resistance is as

$$P = \frac{(K_v V)^2 EI l}{2} \frac{\omega}{1 + \omega^2 \tau^2} \frac{\alpha}{1 + \alpha^2}. \quad (20)$$

The power reaches maximum at  $\omega = 1/\tau$  and  $\alpha = 1$  with the value of

$$P_{\max} = \frac{(K_v V)^2 EI l}{8\tau}, \quad (21)$$

where  $l$  is the length of the strip. The power density is evaluated as  $P_{\max}$  over volume as

$$P_d = \frac{(K_v V)^2 E h^2}{96\tau}, \quad (22)$$

where  $h$  is the thickness of the strip.

The parameters of a TBA<sup>+</sup>/Flemion sample in thickness of 0.17 mm from the AIST, Japan was determined as

$$K_v = 0.0193 \text{ (mmV)}^{-1}, \tau = 76.81 \text{ sec}, E_{eq} = 72 \text{ Mpa.}$$

The power density of this sample is estimated as  $P_d = 0.48 \text{ W/m}^3$  for 2 V peak voltage at frequency of 0.0021 Hz.

Using the same principle, corresponding formulation for IPMC with relaxation can be derived from the four-parameter model, but is not as explicit and simple as that for IPMC without relaxation. An alternative method is to calculate power numerically and find the maximum. A Li<sup>+</sup>/Nafion sample in thickness of 0.196 mm from ERI has parameters of

$$K_{v1} = 0.027 \text{ (mmV)}^{-1}, K_{v2} = 0.01 \text{ (mmV)}^{-1}, \tau_1 = 0.3 \text{ s}, \tau_2 = 11 \text{ s}, E = 240 \text{ MPa}$$

The estimated power density is  $P_d = 870 \text{ W/m}^3$  for 2 V peak voltage input at 0.5 Hz.

## 5. DISCUSSION

IPMC is a group of ionic EAP with performances and materials characteristics that are strongly dependent on the material constituents, fabrication process and history. The performances may vary as a result of ions exchange with the water in which the material is immersed. Therefore, the acquired data, the extracted material parameters and the documented performances that are mentioned in this paper may be meaningful only to the particular samples and the particular test conditions.

In order to characterize the IPMC materials, efforts have been made to develop macro models, which address the electric input and mechanical actuation characteristics of these EAP materials. These models were constructed based on the experimental observation rather than the analysis of the micro physiochemical mechanism. Using the models, we define the parameters of the materials and extract them from experimental data by best-fit algorithm.

Two input models, the simple clumped RC circuit and the distributed RC line were proposed. Experimental data show that the later may be a better expression of the behavior of IPMCs that have fractal-like electrodes. A four-parameter model was developed to represent the actuation response of the IPMC with relaxation. This model fits the relaxation curve very well. These macro models include ordinary differential equations that provide a mathematical tool to calculate the response of the IPMC. By using these equations, we estimated the power density of the IPMCs.

In the derivation of four-parameter actuation model, the simple clumped RC input model was used. This model was not found to provide a good representation of IPMC materials with fractal-like electrodes. Currently, the distributed RC line model is under development and its integration with the actuation model will be explored in a future study.

## ACKNOWLEDGMENTS

The research at Jet Propulsion Laboratory (JPL), California Institute of Technology, was carried out under a Defense Advanced Research Projects Agency (DARPA) contract with the National Aeronautics and Space Agency (NASA). The authors would like to acknowledge the contribution of Flemion based IPMC samples from Dr. Kinji Asaka, National Institute of Advanced Industrial Science and Technology (AIST), as well as Dr. Kazuo Onishi, and Dr. Shingo Sewa, Eamex Corporation, Japan. The Nafion base IPMC was provided from M. Shahinpoor from Environmental Robots Inc. (ERI) that were used to acquire the data.

## REFERENCES

1. Y. Bar-Cohen (Ed.), *Electroactive Polymer (EAP) Actuators as Artificial Muscles - Reality, Potential and Challenges*, pp. 1-671, SPIE Press, Vol. PM98, 2001.
2. S. Sherrit, and Y. Bar-Cohen, "Methods and Testing and Characterization," *Electroactive Polymer (EAP) Actuators as Artificial Muscles - Reality, Potential and Challenges*, Y. Bar-Cohen (Ed.), pp. 405-453, SPIE Press, Vol. PM98, 2001.
3. Y. Bar-Cohen, X. Bao, S. Sherrit, S. Lih, "Characterization of the Electromechanical Properties of Ionomeric Polymer-Metal Composite (IPMC)," Proceedings of SPIE's 9th Annual International Symposium on Smart Structures and Materials, 17-21 March, 2002, San Diego, CA. Paper No. 4695-27, 2002
4. K. Onishi, S. Sewa, K. Asaka, N. Fujiwara, K. Oguro, "Morphology of electrodes and bending response of the polymer electrolyte actuator," *Electrochimica Acta* **46**, 737-743, 2000.
5. S. Nemat-Nasser, and C. Thomas "Ionic Polymer-Metal Composite (IPMC)," Topic 3.2, Chapter 12, "Electroactive Polymer (EAP) Actuators as Artificial Muscles - Reality, Potential and Challenges," *ibid*, pp. 139-191, 2001.
6. K. Onishi, S. Sewa, K. Asaka, N. Fujiwara, K. Oguro, "The effects of counter ions on characterization and performance of a solid polymer electrolyte actuator," *Electrochimica Acta* **46**, pp. 1233-1241, 2001.
7. K. Bhattacharya, J. Li, X. Yu, "Electro-mechanical models for optimal design and effective behavior," *Electroactive Polymer (EAP) Actuators as Artificial Muscles - Reality, Potential and Challenges*, Y. Bar-Cohen (Ed.), pp. 309-330, SPIE Press, Vol. PM98, 2001.